

Low-Energy Singlets in the Heisenberg Antiferromagnet on the Kagome Lattice

Ran Budnik¹ and Assa Auerbach^{1,2}

¹Physics Department, Technion, Haifa 32000, Israel

²The Physics Laboratories, Harvard University, Cambridge, Massachusetts 02138, USA

(Received 25 June 2004; published 29 October 2004)

The spin- $\frac{1}{2}$ Heisenberg antiferromagnet on the kagome lattice, is mapped by contractor renormalization to a spin-pseudospin Hamiltonian on the triangular superlattice. Variationally, we find a ground state with columnar dimer order. Dimer orientation fluctuations are described by an effective O(2) model at energies above an exponentially suppressed clock mass scale. Our results explain the large density of low-energy singlets observed numerically, and the nonmagnetic T^2 specific heat observed experimentally.

DOI: 10.1103/PhysRevLett.93.187205

PACS numbers: 75.10.Jm, 75.10.Hk, 75.30.Ds

Frustrated quantum antiferromagnets (AFM) are important paradigms of emerging phenomena in models of condensed matter. It has long been appreciated that, due to the extensive ground state manifold of the *classical* kagome AFM [1], quantum fluctuations may destroy magnetic order and replace it with paramagnetic phases with novel excitations at low-energy scales.

Numerical studies of the spin- $\frac{1}{2}$ kagome AFM have suggested that its ground state does not support long range spin order [2–4]. The low spectra of finite kagome clusters [5] consist of *singlets* whose number increases exponentially with the lattice size.

Experimentally, there is a mounting evidence of unusual low-energy excitations in kagome like systems. In spin- $\frac{3}{2}$ SrCr₉Ga₁₂O₁₉ [6,7] a significant fraction of the spin moment is *not frozen* below the non linear susceptibility maximum at $T = 5$ K. Recently, muon resonance experiments on a spin- $\frac{1}{2}$ system [8] reported that below the susceptibility maximum of $T = 20$ K, low frequency spin fluctuations were detected but *without static magnetization* down to 50 mK.

However, the specific heat of SrCr₉Ga₁₂O₁₉ has an unexplained large T^2 coefficient which apparently does not arise from spin waves [7].

Thus there is both numerical and experimental evidence that there are seemingly *nonmagnetic* massless modes whose origin has not yet been understood. Weak bonds perturbation theory found that dimer singlets span the low-energy spectrum [9,10], and interesting results have been found for the kagome Quantum Dimer Model [4,11]. However, the Quantum Dimer Model has not yet been quantitatively derived from the Heisenberg model.

It is the purpose of this Letter to elucidate the nature of low-energy excitations of the $S = 1/2$ Kagome AFM by applying the nonperturbative contractor renormalization (CORE) method [12]. CORE has been recently applied to the square lattice Hubbard model [13], Heisenberg ladders [14] (including detailed convergence tests [15]), and the frustrated Checkerboard and Pyrochlore lattices [16].

For the kagome lattice, CORE leads to an effective spin-pseudospin (S-L) model on a triangular lattice. A variational analysis reveals *columnar dimer order* in the spin disordered ground state, and low-energy excitations which can be understood as dimer orientation fluctuations. We describe these fluctuations by a $p = 6$ quantum clock model. Its mass gap is strongly suppressed by quantum fluctuations by a factor estimated at about 10^{-4} . Thus, the low-energy singlet spectrum is in effect a quasi Goldstone mode of an O(2) order parameter. The number of sub gap singlets increases exponentially with lattice size and gives rise to a T^2 specific heat as seen experimentally.

The Heisenberg Hamiltonian on the kagome lattice, (see Fig. 1), is

$$H = J \sum_{\langle ij \rangle} \mathbf{S}_i \cdot \mathbf{S}_j; \quad (1)$$

Henceforth we set the unit of energy to $J = 1$.

Blocks.—CORE involves (i) an initial choice of elementary blocks which cover the lattice, and (ii) a truncated set of block eigenstates whose tensor product spans the reduced Hilbert space. It is useful to choose minimally sized blocks which respect (as much as possible) the lattice point group symmetry. Here we select upward

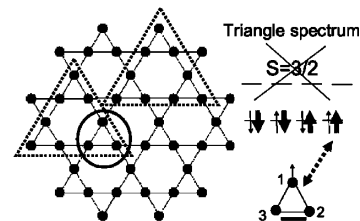


FIG. 1. CORE on the kagome lattice (solid circles). Triangular blocks of first (second) CORE steps are encircled by solid (dashed) lines. On the right: triangle four ground states are labeled by spin (arrows) and pseudospins (wide arrows). The $\uparrow\uparrow$ state of the triangle is visualized as a dimer singlet on the bottom rung.

triangles, and a truncated basis of the four degenerate spin half ground states, discarding the higher $S = 3/2$ states, (see Fig. 1).

The S-L representation of the four ground states are labeled by $|s, l\rangle$, where $s = \uparrow, \downarrow$ is the magnetization and $L^z = l = \uparrow, \downarrow$ is the pseudospin in the z direction. Explicitly, in the Ising basis $|s_1 s_2 s_3\rangle$,

$$\begin{aligned} |s, \uparrow\rangle &= \frac{(|s\uparrow\downarrow\rangle - |s\downarrow\uparrow\rangle)}{\sqrt{2}} \\ |s, \downarrow\rangle &= \frac{|s\uparrow\downarrow\rangle + |s\downarrow\uparrow\rangle}{\sqrt{6}} - \sqrt{\frac{2}{3}}|(-s)ss\rangle. \end{aligned} \quad (2)$$

The pseudospin direction in the xz plane correlates with the direction of the singlet bond, e.g. \uparrow describes a singlet dimer on the bottom ($-\hat{z}$) edge (see Fig. 1). Thus, the L^y eigenstates have definite chiralities.

Effective Hamiltonian.—The effective interactions between triangles is calculated by CORE [12,13]. We note that this approach is feasible when two conditions are met: (i) Interaction matrix elements fall off rapidly with range such that the truncation error at finite ranges is small, and (ii) the norms of the projected eigenstates are sufficiently large for numerical accuracy. We have computed all range 2 and range 3 interactions, and neglected range 4 corrections, whose expectation values were found to be an order of magnitude smaller. At range 3, norms of projected eigenstates were greater than 0.75, with most states above 0.9.

The effective Hamiltonian is a spin-pseudospin (S-L) Model on the triangular lattice:

$$\begin{aligned} \mathcal{H}_{\text{SL}} &= \mathcal{H}_{ss} + \mathcal{H}_{ll}, \\ \mathcal{H}_{ss} &= \sum_{\langle ij \rangle} \mathbf{S}_i \cdot \mathbf{S}_j [J_{ss} + J_{sslele}(\mathbf{L}_i \cdot \mathbf{e}_{ij}) \cdot (\mathbf{L}_j \cdot \mathbf{e}_{ji}) \\ &\quad + J_{ssll}(\mathbf{L}_i^\perp \cdot \mathbf{L}_j^\perp) + J_{ssle1}(\mathbf{L}_i \cdot \mathbf{e}_{ij}) \\ &\quad + J_{ssle2}(\mathbf{L}_j \cdot \mathbf{e}_{ji}) + J_{sslyly} \mathbf{L}_i^y \mathbf{L}_j^y], \\ \mathcal{H}_{ll} &= J_{lele}(\mathbf{L}_i \cdot \tilde{\mathbf{e}}^{ij}) \cdot (\mathbf{L}_j \cdot \tilde{\mathbf{e}}_{ji}) + J_{ll}(\mathbf{L}_i^\perp \cdot \mathbf{L}_j^\perp) \\ &\quad + J_{lyly} \mathbf{L}_i^y \mathbf{L}_j^y. \end{aligned} \quad (3)$$

Here $\mathbf{L}^\perp = (\mathbf{L}^x, \mathbf{L}^z)$, and $\mathbf{e}_{ij}, \mathbf{e}_{ij}^l$ are unit vectors in the xz plane. \mathcal{H}_{ss} describes interactions of the Kugel-Khomskii type [10,17], where the pseudospin exchange anisotropy depends on the sites and bond directions. (See Fig. 2). For any other other bond $\langle ij' \rangle$, $\mathbf{e}_{ij'}$ is simply found by rotating \mathbf{e}_{ij} by $0, \pm 120^\circ$ according to the $O(2)$ rotation of $\langle ij \rangle \rightarrow \langle ij' \rangle$.

The coupling constants and angles of \mathcal{H}_{SL} , are tabulated in Table I. Missing from (3) are terms which vanish in the periodic lattice by summation over nearest neighbors, and three site (ring exchange) interactions. The largest term $K \mathbf{S}_i \cdot \mathbf{S}_j L_i^z L_j^z L_k^z$ has a largest matrix element of magnitude 0.02.

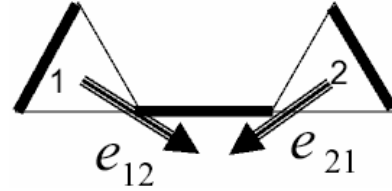


FIG. 2. CORE range 2. Directions of anisotropy vectors $\mathbf{e}_{ij} = \mathbf{e}_{ij}^l = \tilde{\mathbf{e}}_{ij}$ for a horizontal bond. For other bond directions, vectors must be rotated by $\pm 120^\circ$. The ground state singlet correlations of two coupled blocks are depicted by thick lines.

While \mathcal{H}_{SL} may prove to be useful for numerical studies of the spectrum of larger lattices, its complexity somewhat obscures its physics. It is simple however to study \mathcal{H}_{SL} variationally (i.e. classically) using pseudo-spin coherent states [18] $\psi[s] \prod_i |s_i, l_i\rangle$ where $\mathbf{L} \cdot \mathbf{l} |s, l\rangle = \frac{1}{2} |s, l\rangle$. Its energy $E^{\text{var}}[l] = \sum_{ij} \langle \mathbf{S}_i \mathbf{S}_j \rangle_{[l]} F[l] + E_{ll}[l]$ is minimized with respect to the directions l_i .

We start by evaluating the energy of the magnetically ordered state, where both the spins and the pseudospins form three sublattice (3SL) Néel order on the triangular lattice (and $\sqrt{3} \times \sqrt{3}$ order on the kagome). Other candidates are the dimer coverings of two triangle singlets, whose correlations are defined by Fig. 2. The dimer singlet states have been shown by Mila and Mambrini [10] to span much of the low singlet spectrum in finite cluster calculations. The variational analysis highlights the special role of the “dimerization fields”, J_{ssle1}, J_{ssle2} in (3), for the formation of local singlets. These terms cancel under summation in all uniform states defined by $\langle \mathbf{S}_i \mathbf{S}_j \rangle = \text{const}$. Their significant magnitude (see Table I) helps to lower the energy considerably by aligning l_i with the anisotropy vectors \mathbf{e}_{ij} to form singlets on certain bonds and not others $\langle \mathbf{S}_i \mathbf{S}_j \rangle = -\frac{3}{4} \delta_{\langle ij \rangle \text{dim}}$. This is a strong argument in favor of a nonmagnetic ground state. Consequently, \mathcal{H}_{ll} is crucial in selecting the true ground state among the multitude of dimer singlet coverings. We have found that the perfectly ordered *columnar dimer* (CD) state minimizes \mathcal{H}_{ll} . A local “defect” of a rotated dimer in the CD background costs a “twist” energy of +0.01 per site.

In Fig. 3 we depict the 3SL and CD states. Their energies per site are

$$E_{\text{CD}}/\text{site} = -0.229, \quad E_{3\text{SL}}/\text{site} = -0.178, \quad (4)$$

TABLE I. CORE up to range 3: Interaction parameters for the effective Hamiltonian \mathcal{H}_{SL} , Eq. (3). Underlined are the dimerization fields (see text).

J_{ss}	J_{sslele}	J_{ssll}	J_{ssle1}	J_{ssle2}	J_{sslyly}	\mathbf{e}_{12}	\mathbf{e}_{21}
0.108	0.954	0.211	0.281	0.278	0.053	113°	248°
J_{lele}	J_{ll}	J_{lyly}	\mathbf{e}_{12}^l	\mathbf{e}_{21}^l			
0.060	-0.001	0.038	132°	222°			

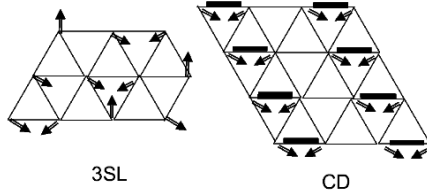


FIG. 3. Variational states on the triangular superlattice: The 3SL and the CD state; arrows denote pseudospins, and thick lines denote singlet dimers.

where the evaluation uses the known spin correlations of the Heisenberg AFM on the triangular lattice [19] $\langle \mathbf{S}_i \mathbf{S}_j \rangle = 0.18$.

This result can be connected to numerical diagonalizations data as follows. The number of quasi degenerate CD states on Kagome clusters with the lattice group symmetry is 24: From a particular up-triangle site there are six dimer directions. There are two equivalent dimer orderings of the neighboring lines of dimers. Another factor of 2 is given by the down triangle configurations. Between these 24 CD states there are exponentially vanishing overlaps at large lattices.

Quantum Clock Model.—A continuum Hamiltonian for the low-energy fluctuations is derived as follows. Using the subset of site positions \mathbf{x} belonging to a 2×2 superlattice (see Fig. 4), every dimer configuration defines a unique configuration of sixfold clock angles $\phi(\mathbf{x})$'s defining the orientations of dimers from the selected sites.

A ferromagnetic state of ϕ 's represents a CD ground state (up to global translations, with vanishing overlap, of an interpolating line of dimers). The resistance to local twists, governed by J_{lel} , is described by energy density $\frac{1}{2} \rho_s (\nabla \phi)^2$, $\rho_s \approx 0.01$. The barrier height between dimer orientations is estimated from Eq. (4) to be $h_6 = 0.05$ which defines the ‘‘clock field’’ $h_6 \cos(6\phi)$. $J_{lyly} L_y L_y$ interactions rotate the pseudospins and the dimers in the plane, giving rise to a kinetic energy $\frac{1}{2} \chi \dot{\phi}^2$, $1/\chi \approx 0.01$.

$$h_6 \int \mathcal{D}\phi_{>} \cos[p(\phi_{<} + \phi_{>})] \exp\left(-\frac{1}{2} \phi_{>} G^{-1} \phi_{>}\right) = h_6 \cos(p\phi_{<}) e^{-p^2 \langle \phi_{>}^2 \rangle}, \quad h_6^{\text{ren}} = h_6 e^{-Cp^2} \approx 0.05 \times 10^{-4} \quad (6)$$

Our rough numerical evaluation of $C \approx 0.2$ uses the zero point phase fluctuations of an effective spin-2 quantum xy model, describing four pseudospin half in the unit cell. Equation (6) is our key result: tunnelling between $p = 6$ ground states renormalizes down the clock mass gap by a Gaussian function of p . In particular, the dispersion of ϕ fluctuations

$$\omega_{\mathbf{q}}^{S=0} = \sqrt{(h_6^{\text{ren}})^2 + \frac{\rho_s}{\chi} |\mathbf{q}|^2} \quad (7)$$

resembles Goldstone modes of an $O(2)$ xy model at frequencies and temperatures larger than (6). In this regime, the singlets' contribution to the specific heat C_V and entropy S is quite large. Using thermodynamics of free

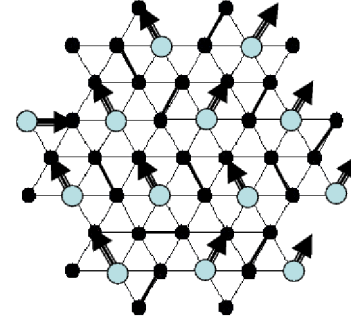


FIG. 4 (color online). Clock fields $\phi(\mathbf{x})$ (thick arrows) defined by the dimer directions from the sites marked by large circles.

Thus we arrive at a long wavelength partition function of a (2+1)D quantum clock model which describes the lowest singlet sector of the kagome spectrum:

$$Z_{\text{singlets}} = \int \mathcal{D}\phi \exp\left(-\int_0^\beta d\tau d^2\mathbf{x} \left[\frac{1}{2} \chi \dot{\phi}^2 + \frac{1}{2} \rho_s (\nabla \phi)^2 + h_6 \cos(6\phi) \right]\right) \quad (5)$$

The renormalization group analysis of José *et al.* [20] for the classical p -state clock model in two dimensions found that at low temperatures $T < T_p = 8\pi/p^2$ the clock field h_p is a relevant interaction which locks the ground state into a clock minimum, with a finite gap for domain wall excitations. For our quantum clock model the clock term is still relevant, but quantum fluctuations, which involve tunnelling between clock minima, drastically renormalize down the value of the clock field and the mass gap for the long wavelength excitations.

This is shown as follows: we expand the action of (5) to lowest order in $h_6 \cos(6\phi)$ and integrate out the high momenta and energy modes $\phi_{>}$

bosons, we obtain

$$C_V \sim \frac{\chi}{\rho_s} T^2, \quad S(E) \sim N \left(\frac{E}{N0.01} \right)^{2/3}, \quad (8)$$

where N is the number of effective sites, and E the total energy. Thus, the smallness of h_6^{ren} provides the long sought after explanation of the unusual exponential proliferation of singlets at sub gap energies [5]. In addition, the singlets pseudo Goldstone mode may now explain the experimentally reported T^2 term in the specific heat [7].

We note that the CD state has no long range spin order. The spin gap can be estimated from the variational energy difference between CD and 3SL states to be of the order of

TABLE II. Second CORE iteration: Interaction parameters for \mathcal{H}_{SL} evaluated up to range 2.

J_{ss}	J_{sslele}	J_{ssll}	J_{ssle_1}	J_{ssle_2}	J_{sslyly}	\mathbf{e}_{12}	\mathbf{e}_{21}
0.113	0.08	-0.005	0.026	0.182	-0.039	330°	280°
J_{lele}	J_{ll}	J_{lyly}	\mathbf{e}'_{12}	\mathbf{e}'_{12}			
-0.019	-0.003	0.004	200°	160°			

$h_6 = 0.05$. Another estimate can be obtained by iterating CORE on H_{SL} .

At the second CORE step, the triangular lattice is covered by triangles (which are blocks of nine kagome lattice sites). These form a triangular superlattice with directed bonds (see Fig. 1). For both the Heisenberg and \mathcal{H}_{SL} , each block has four degenerate $S = 1/2$ ground states which can again be represented by a spin and a pseudospin. The second CORE step thus maps the S-L Hamiltonian (3) onto itself with new interaction parameters and anisotropy vectors, as listed in Table II.

What can we learn from step 2?

In contrast to the first CORE step (see Table I), the vectors $\mathbf{e}_{ij} \cdot \mathbf{e}_{ji} > 0$, i.e., ferromagnetic. J_{sslele} has decreased while J_{ss} did not. Thus the Hamiltonian prefers local singlet correlations with aligned pseudospins, which is consistent with columnar order.

Spin gap.—By iterating CORE we can compute the splitting between the $S = \frac{1}{2}$ ground state and the lowest $S = \frac{3}{2}$ excitation on triangular clusters. At second iteration, the spin gap deduced for 81 original kagome lattice sites is 0.06. CORE breaks down at the third step, where many of the wave function overlaps vanish. This is expected due to the onset of long range CD order, since states with high pseudospin parentage have lower energy. Stopping at 81 sites, we can only observe that while the spin gap is larger than the dimer fluctuations bandwidth, there is no conclusive sign of saturation to a finite thermodynamic limit.

In summary, we have computed the effective Hamiltonians of the $S = 1/2$ Heisenberg antiferromagnet on the kagome lattices using CORE up to range 3. Variationally, we conclude that the kagome lattice has long range columnar dimer order and a very low gap for singlet excitations in the thermodynamic limit. CD order might induce experimentally detectable lattice distortions. Further details can be found elsewhere [21].

Discussions with E. Altman, E. Demler, C. Lhuillier, and D. Nelson are gratefully acknowledged. A. A. is thankful for the hospitality of Harvard University, Aspen Center for Physics, and Kavli Institute for Theoretical Physics where part of this work has been completed. This work was supported in part by the US-Israel Binational Science Foundation.

*In a recent preprint, Capponi, Laeuchli, and Mambrini [22] have independently computed \mathcal{H}_{SL} of Eq. (3) by CORE, and found excellent numerical agreement with large cluster diagonalizations.

- [1] V. Elser, Phys. Rev. Lett. **62**, 2405 (1989); S. Sachdev, Phys. Rev. B **45**, 12377 (1992); J. von Delft and C. L. Henley, Phys. Rev. B **48**, 965 (1993).
- [2] C. Zeng and V. Elser, Phys. Rev. B **42**, 8436 (1990).
- [3] J. T. Chalker and J. F. G. Eastmond, Phys. Rev. B **46**, 14201 (1992).
- [4] review in G. Misguich and C. Lhuillier, *Frustrated Spin Systems*, edited by H. T. Diep, (World-Scientific, Singapore, 2003) and references therein.
- [5] P. Lecheminant, B. Bernu, C. Lhuillier, L. Pierre, and P. Sindzingre, Phys. Rev. B **56**, 2521 (1997); C. Waldtmann, H.-U. Everts, B. Bernu, C. Lhuillier, P. Sindzingre, P. Lecheminant, and L. Pierre, Eur. Phys. J. B **2**, 501 (1998).
- [6] C. Broholm *et al.*, Phys. Rev. Lett. **65**, 3173 (1990); A. Keren *et al.*, Phys. Rev. B **53**, 6451 (1996).
- [7] A. P. Ramirez *et al.*, Phys. Rev. Lett. **64**, 2070 (1990); B. Martínez *et al.*, Phys. Rev. B **46**, 10786 (1992); A. P. Ramirez *et al.*, Phys. Rev. Lett. **84**, 2957 (1999).
- [8] A. Fukaya *et al.*, Phys. Rev. Lett. **91**, 207603 (2003).
- [9] A. V. Syromyatnikov and S. V. Maleyev, Phys. Rev. B **66**, 132408 (2002).
- [10] F. Mila, Phys. Rev. Lett. **81**, 2356 (1998); M. Mambrini and F. Mila, Eur. Phys. J. B **17**, 651 (2000).
- [11] D. S. Rokhsar and S. A. Kivelson, Phys. Rev. Lett. **61**, 2376 (1988); R. Moessner, S. Sondhi, and E. Fradkin, Phys. Rev. B **65**, 24504 (2002); G. Misguich, D. Serban, and V. Pasquier, Phys. Rev. Lett. **89**, 137202 (2002); P. Nikolic and T. Senthil, Phys. Rev. B **68**, 214415 (2003).
- [12] C. Morningstar and M. Weinstein, Phys. Rev. D **54**, 4131 (1996).
- [13] E. Altman and A. Auerbach, Phys. Rev. B **65**, 104508 (2002).
- [14] J. Piekarewicz and J. R. Shepard, Phys. Rev. B **56**, 5366 (1997); J. Piekarewicz and J. R. Shepard, Phys. Rev. B **57**, 10260 (1998).
- [15] S. Capponi and D. Poilblanc, Phys. Rev. B **66**, 180503 (2002).
- [16] E. Berg, E. Altman, and A. Auerbach, Phys. Rev. Lett. **90**, 147204 (2003).
- [17] K. I. Kugel and D. I. Khomskii, Sov. Phys. Usp. **25**, 231 (1982).
- [18] A. Auerbach, *Interacting Electrons and Quantum Magnetism*, (Springer-Verlag, NY, 1994).
- [19] L. Capriotti, Int. J. Mod. Phys. B **15**, 1799 (2000).
- [20] J. V. José, L. P. Kadanoff, S. Kirkpatrick, and D. R. Nelson, Phys. Rev. B **16**, 1217 (1977).
- [21] R. Budnik, M.Sc. thesis, Technion, 2004.
- [22] S. Capponi, A. Laeuchli, and M. Mambrini, Phys. Rev. B **70**, 104424 (2004). Differences in spin gap values are due to different range 3 corrections.